Ageing of 100Cr6 steel: synchrotron X-ray diffraction and dimensional analysis investigation

V. Lejay[1,2], C. Sidoroff[2], C. Le Bourlot[1], M. Perez*[1] and P. Dierickx[2]

Thermal ageing of 100Cr6 with different initial austenitisings was studied using the combination of synchrotron X-ray diffraction and dimensional variation measurements. Synchrotron X-ray diffraction provided the phase volume fractions and their carbon content through the analysis of the lattice parameters. Dimensional measurements were obtained *in situ* in a quench dilatometer also used to realise the heat treatment. The combined analysis of these data provides a better understanding of phase evolutions. For the different austenitising treatments investigated, the dimensional variations were found to be easily linked to the phase parameters measured by X-ray diffraction.

Keywords: 100Cr6 steel, AISI 52100 steel, Martensite ageing, X-ray diffraction, Dimensional analysis, Carbides

Introduction

In bearing applications, steels must present high hardness to ensure long rolling contact fatigue lives in service.[1] 100Cr6 steel is widely used by bearing manufacturers in a quenched and tempered state. In such a state, the microstructure obtained is composed of metastable constituents that may evolve in service inducing potentially detrimental dimensional variations: loss of fit, clearance variation.[2–6] It is possible to realise a stabilising tempering by increasing the tempering temperature, but the hardness as a consequence will be reduced.

To optimise the heat treatment and get the best hardness/dimensional stability compromise, it is therefore important to predict microstructural evolutions and their related dimensional variations.

Tempering of steels,[7–9] and especially of 100Cr6, and its dimensional consequences,[2–5] have been extensively studied in the literature. A recent study conducted by the authors[10] presented an original approach coupling experimental ageing characterisation of the microstructure by thermo-electric power measurements and a modelling of the ageing evolutions to predict macroscopic dimensional variations. However, all above-mentioned studies suffered from the lack of information on the exact carbon content of martensite and austenite, as well as the precise knowledge of phase fractions.

The aim of this work is to use synchrotron source X-ray diffraction (XRD) to determine phase volume fraction and phase carbon content,[11] in combination with *in situ* dimensional analysis, to better understand complex dimensional variations occurring during ageing after different initial austenitising heat treatments.

Materials, treatments and techniques

100Cr6 bearing steel and treatments

All experiments were realised on 100Cr6 samples machined from one steel batch with a carbon composition of 0.96 wt-% and chromium composition of 1.41 wt-%. Four initial heat treatments were studied consisting of various austenitizing temperatures and times, namely (1) 10 minutes at 880°C, (2) 10 minutes at 850°C, (3) 30 minutes at 850°C and (4) 10 minutes at 820°C. These treatments were performed in a DIL-805 quench dilatometer (see next section) and followed by rapid cooling to simulate an oil quench. These treatments were followed by isothermal ageing treatments performed at 170 and 230°C during up to 10 000 seconds.

In situ dimensional analysis

A DIL-805 quench dilatometer from TA Instruments was used to assess *in situ* dimensional variations on cylindrical samples (diameter: 4 mm, length: 10 mm) during isothermal ageing, following austenitizing and quenching.

To reach the ageing temperature, a heating rate of 10°C s^{-1} was selected so as to avoid both temperature overshoot and substantial phase evolution during heating. Despite this high heating rate, the contraction associated to carbon precipitation from supersaturated martensite is initiated during the heating; hence the initial length L_0 at the beginning of ageing cannot be directly obtained. Therefore, it has been set as the length of the sample at 170 and 230°C during the first heating up to austenitizing temperature.

[1]Univ. Lyon – INSA Lyon – MATEIS, UMR CNRS 5510 – F69621, Villeurbanne, France
[2]NTN-SNR Roulements, 1 rue des Usines, 74 000 Annecy, France

*Corresponding author, email Michel.Perez@insa-lyon.fr

Published by Taylor & Francis on behalf of the Institute
Received 1 September 2015; accepted 8 December 2015
DOI 10.1080/02670836.2015.1136102

X-ray diffraction at the synchrotron

XRD is used to estimate lattice parameters and phase fractions. The advantage of synchrotron sources is the possibility to study the sample in transmission mode and also to obtain high-resolution diffractograms.

Discs of thickness 0.7 mm were cut out of the dilatometer cylinders with precautions, and submitted to ageing treatments of 0, 10, 100, 1000 or 10 000 seconds at 230°C.

All samples were studied on beamline ID11 at the ESRF to monitor peak variations. The non-aged samples were also analysed on beamline ID22 to characterise precisely the initial state. ID22 uses a high-resolution powder diffractometer (energy of 42 KeV), acquisition time is 45 minutes per sample. ID11 uses a 2D detector and (energy of 59 KeV), acquisition time is a few seconds per sample. Calibration and instrument broadening are determined using CeO_2 and Si powders.

Because of a very low texture, the 2D-diffraction patterns were integrated along the radius to obtain a 1D-diffractogramm. A Rietveld refinement was performed on all the spectrograms using the Maud software[12] in batch mode. The input parameters were instrumental broadening and basic phase parameters. The output data were the phase fractions and lattice parameters for martensite, austenite and cementite.

Results

Phase fractions and composition from XRD

Lattice parameters of martensite and austenite can be related to carbon content in solid solution. Carbon provides martensite its tetragonal structure, visible in XRD through peak splitting. In austenite, carbon increases the distance between iron atoms, resulting in a peak shifting.

Many relationships can be found in literature concerning the lattice parameter dependence of martensite upon carbon content. Xiao *et al.*[13] present various existing data gathered by Roberts.[14] More recent and accurate data gathered by Cheng *et al.*[15] led to the following equation:

$$\left(\frac{c}{a}\right)_{\alpha} = 1 + 0.045[\mathrm{C}]_{\alpha}^{\mathrm{wt}} \quad (1)$$

where c and a are the lattice parameters of martensite (in Angstrom), and $[\mathrm{C}]_{\alpha}^{\mathrm{wt}}$ is the carbon solute content in ferrite (in wt-%). It is assumed here that other alloying elements (such as Cr and Mn) do not change significantly the lattice parameter of iron.[11,16]

The advantage of using the c/a ratio is that experimental error is reduced because the relationship only requires the angle difference between the split peaks (visible for peak {220}α in Fig. 1), the absolute peak position is not needed.

Retained austenite has a cubic structure and austenite carbon content $[\mathrm{C}]_{\gamma_R}^{\mathrm{wt}}$ can only be estimated through absolute peak position using the following equation[11]:

$$a_{\gamma_R} = 3.556 + 0.0453[\mathrm{C}]_{\gamma_R}^{\mathrm{wt}} \quad (2)$$

Figure 2 presents the output data of the Rietveld analysis of the XRD results, and its translation in carbon concentration and phase fraction. As expected, increasing the austenitizing conditions (time or temperature), by

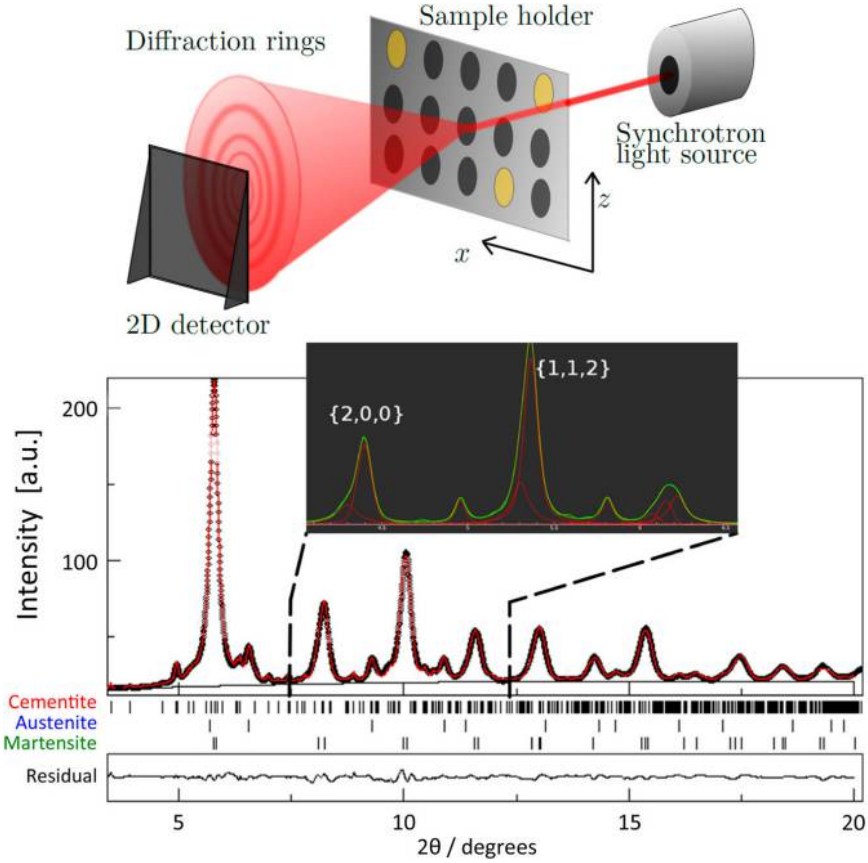

1 Schematic of sample mounting system and ID11 and ID22 beam lines, and typical diffractogram obtained and analysed with Rietveld refinement, showing a doublet for {200}α

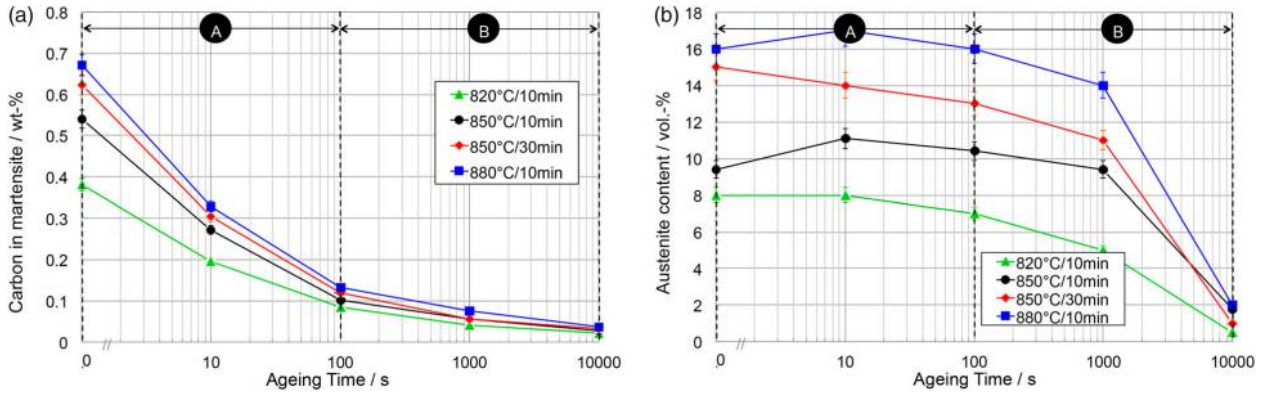

2 Output data of Rietveld analysis: *a* carbon content in martensite, *b* retained austenite volume fraction as a function of ageing times at 230°C. Stages A and B refer to the precipitation of *ε*-carbides and cementite, respectively (see Perez *et al.*[10] for more details)

allowing a higher dissolution of carbides in the Fe-matrix, leads to higher initial retained austenite contents (8–16 vol.-%) and to a higher carbon content in martensite (from 0.4 to 0.7 wt-%).

In the following, Stages A and B refer to the precipitation of ε-carbides and cementite, respectively (as defined in Perez *et al.*[10]). During ageing, carbon precipitation from martensite is visible through the decrease of carbon content in martensite: a large decrease during Stage A, and a slower decrease during Stage B until no carbon remains in the martensite. Retained austenite volume fraction remains constant during Stage 1 and drops down to zero during Stage 2, in agreement with Perez *et al.*[10]

The total carbon concentration of the steel $[C]^{wt}_{total}$ can be estimated assuming that the concentration of carbon in austenite $[C]^{wt}_{\gamma}$ before quench is equal to the concentration of carbon in retained austenite $[C]^{wt}_{\gamma_R}$ after quench:

$$\begin{aligned}(\text{before quench})\,[C]^{wt}_{total} &= [C]^{wt}_{\gamma} f^{wt}_{\gamma} + [C]^{wt}_{\theta} f^{wt}_{\theta} \\ &= [C]^{wt}_{\gamma_R}\left(f^{wt}_{\gamma_R} + f^{wt}_{\theta}\right) \\ &\quad + [C]^{wt}_{\theta} f^{wt}_{\theta} \end{aligned} \tag{3}$$

where $[C]^{wt}_{\theta}$ is the weight carbon concentration in cementite and $f^{wt}_{\gamma_R}, f^{wt}_{\alpha}$ and f^{wt}_{θ} are the mass fractions of retained austenite, martensite and cementite, respectively. From XRD measurements, a value of $[C]^{wt}_{total} = 0.97$wt-% is found. This value is in very good agreement with the nominal concentration of the steel (0.96 wt-%, see '100Cr6 bearing steel and treatments' section) measured by spectrometry, giving confidence do the XRD measurements and analysis.

The carbon repartition in each phase is then calculated by summing the carbon content of each phase weighted with the corresponding phase mass fraction f^{wt}:

$$\begin{aligned}(\text{after quench})\,[C]^{wt}_{total} &= [C]^{wt}_{\alpha} f^{wt}_{\alpha} + [C]^{wt}_{\gamma_R} f^{wt}_{\gamma_R} \\ &\quad + [C]^{wt}_{\theta} f^{wt}_{\theta} + [C]^{wt}_{seg} \end{aligned} \tag{4}$$

where $[C]^{wt}_{seg}$ is the residual mass fraction of carbon that is not seen by XRD, which can be calculated subtracting equations (3) and (4). Indeed, the balance of carbon after quench using XRD data does not lead to the total carbon content of 0.96 wt-%: up to 0.2 wt-% is not accounted for (not visible by XRD). It is assumed to be segregated on defects (*e.g.* dislocations, grain boundaries), or present in phases not visible in the diffractograms (*e.g.* alloy carbides, ε-carbide).

These carbon repartitions are represented in Fig. 3, for all treatments in the as-quenched state and for the reference treatment in different states (before quench, as-quenched and aged states). It can be observed in Fig. 3*a*, that increasing austenitizing conditions (time or temperature) also decreases the amount of carbon segregated to defects, that did not stay in the martensite during quench: that is probably due to the fact that low austenitizing

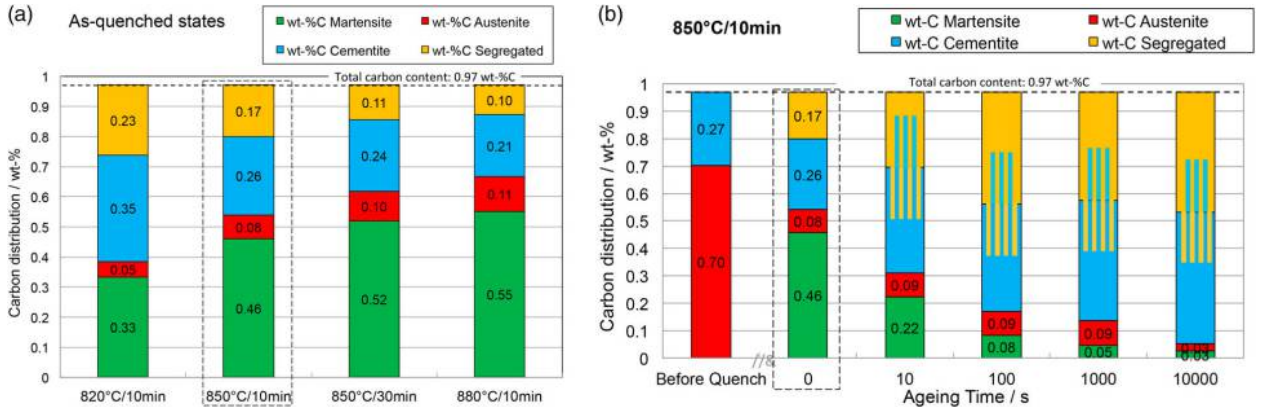

3 Distribution of carbon in the different microstructural constituents according to XRD analysis – *a* as-quenched states after various austenitizing treatments; *b* 850°C/10 minutes state: before quench, and as a function of ageing time at 230°C

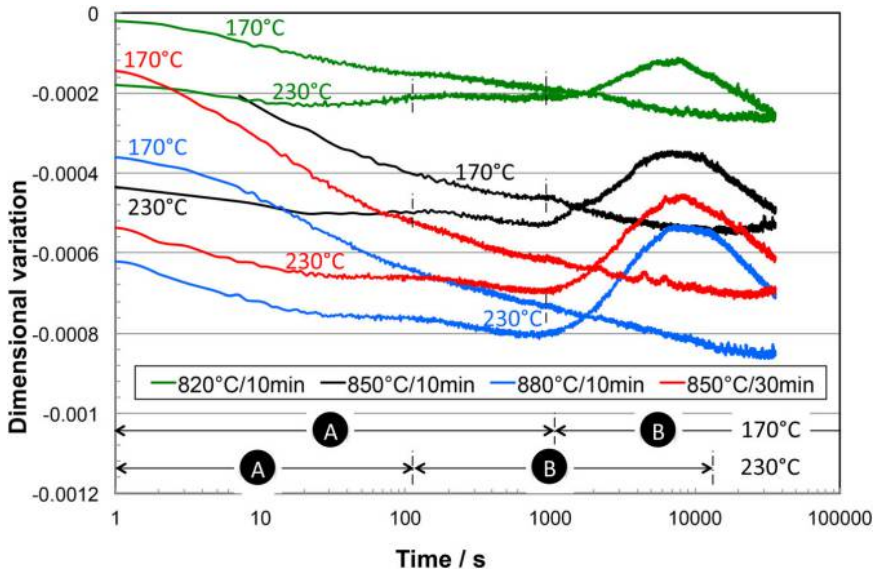

4 Dimensional variation as a function of ageing time at 170 and 230°C – Stages A and B are labelled on the graph with the corresponding time ranges for each ageing temperature. Note that dimensional variations occur during heating and also during the first second of isothermal holding

conditions lead to a finer austenite grain size, and a larger density of lath boundaries and dislocations after quench.

In Fig. 3*b*, it can be observed that most of the carbon either goes to carbides and/or segregates to defects during ageing. Note the relatively high values of the uncertainties of the carbon repartition between segregation and cementite: this is due to the multitude of cementite diffraction peaks combined to the small size of cementite precipitates appearing during ageing.[10]

Dimensional analysis

The dimensional evolutions as a function of ageing time at 170 and 230°C are reported in Fig. 4. In the 170°C ageing, only a contraction is observed. It is due to the precipitation of carbides from martensite occurring in Stage A: the contraction of the martensite matrix due to carbon impoverishment is only partially compensated by the formation of carbides.[17,10] For the 230°C ageing, it is possible to observe the total dimensional evolution kinetics: contraction during Stage A, and an expansion taking over the contraction during Stage B associated to the change of balance between the contraction part (carbon leaving martensite) and the expansion part (carbide formation and retained austenite decomposition). For longer times (above 10 000 seconds) at 230°C, contraction is again observed associated to recovery and/or martensite carbon depletion.

The dimensional variation measured were then analysed using the microstructural data obtained by XRD (see Fig. 5).

For Stage A (Fig. 5*a*), the contraction occurring during Stage A seems to be well related to the initial carbon content in martensite. That seems rather logical since carbon precipitation from martensite is the main contributor to contraction.

For Stage B (Fig. 5*b*), the maximal expansion shows a linear relationship with the initial retained austenite content. That confirms that in the past, simple design rules existed in the literature linking the initial retained austenite content to the maximal dimensional expansion in service.[5] However, this simple rule may not be valid for any thermal treatment, since dimensional variations are a

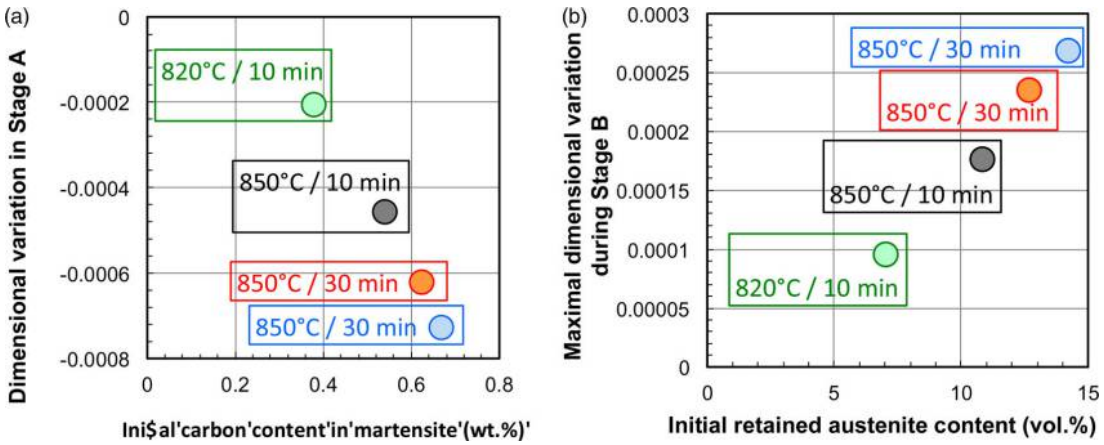

5 Correlation between dimensional variation measured *in situ* at 230°C and data obtained by XRD

complex combination of contractions and expansions. For accurate predictions of dimensional variations, a microstructural model would be needed to estimate phase volume fraction, carbon concentration in both martensite and austenite as a function of ageing time.

Conclusions

An original combination of experimental methodologies have been presented in order to evaluate the microstructural evolutions of 100Cr6 steel when submitted to different quenching and ageing treatments. The use of XRD enables a precise estimation of the carbon content in martensite and in austenite, and of the phase volume fraction. The influence of initial heat treatment was characterised. Even though simple relationships seem to exist between microstructural parameters such as carbon content and phase volume fraction, and dimensional variations during ageing, the problem is complex, and an analytical model is still needed to better design heat treatments and get the best hardness/dimensional stability.

Acknowledgements

The authors thank Jonathan Wright and Andy Fitch of lines ID11 and ID22, for their availability and support during the experimental work at ESRF. Daniel Acevedo and Pascal Daguier from ABS are gratefully acknowledged for realising the quench dilatometer experiments.

References

1. E. V. Zaretsky: '*STLE life factors for rolling bearings*', 1992, Park Ridge, Society of Tribologists and Lubrication Engineers.
2. P. K. Pearson: 'Size change of through hardened bearing steels at application temperatures', *SAE Trans. A*, 1997, **106**, 170–175.
3. P. Duval, G. Murry and A. Constant: 'Stabilité dimensionnelle dans le temps. Contribution à l'étude des facteurs métallurgiques affectant la stabilité dimensionnelle des aciers', *Mécanique Electricité.*, 1968, **11**, 28–37.
4. F. Hengerer, W. Nierlich, J. Volkmuth and H. Nutzel: 'Dimensional stability of high carbon bearing steels', *Ball Bearing J.*, 1988, **231**, 26–31
5. F. Peilloud and M. Guillot: 'Contribution à l'étude de la stabilité dimensionnelle des aciers à roulements', *Mécanique Matériaux Electricité*, 1976, **316**, 28–35.
6. J. Franklin, P. Hill and C. Allen: 'The effect of heat treatment on retained austenite in a 1% carbon/chromium steel', *Heat Treat. Met.*, 1979, **6**, 46–50.
7. G. R. Speich and K. A. Taylor: '*Tempering of ferrous martensites. Martensite: a tribute to Morris Cohen*', 1992, Materials Park, ASM International. 243–275.
8. D. A. Porter and K. E. Easterling: '*Phase transformations in metals and alloys*', 1992, London, Chapman and Hall.
9. C. S. Roberts, B. L. Averbach and M. Cohen: 'The mechanism and kinetics of the first stage of tempering', *Trans. ASM*, 1953, **45**, 576–604.
10. M. Perez, C. Sidoroff, A. Vincent and C. Esnouf: 'Microstructural evolution of martensitic 100Cr6 bearing steel during tempering: from thermoelectric power measurements to the prediction of dimensional changes', *Acta Mater.*, 2009, **57**, 3170–3181.
11. E. Jimenez-Melero, R. Blondé, M. Y. Sherif, V. Honkimäki and N. H. van Dijk: 'Time-dependent synchrotron X-ray diffraction on the austenite decomposition kinetics in SAE 52100 bearing steel at elevated temperatures under tensile stress', *Acta Mater.*, 2013, **61**, 1154–1166.
12. L. Lutterotti, S. Matthies and H.-R. Wenk, 'MAUD (material analysis using diffraction): a user friendly Java program for Rietveld texture analysis and more'. In 'Proceeding of the Twelfth International Conference on Textures of Materials (ICOTOM-12)', **1599**, 1999, Ottowa, NRC Research Press.
13. L. Xiao, Z. Fang, Z. Jinxiu, Z. Mingxing, K. Mokuang and G. Zhenqi: 'Lattice-parameter variation with carbon content of martensite. I. X-Ray diffraction experimental study', *Phys. Rev. B*, 1995, **52**, 9970–9978.
14. C. S. Roberts: 'Effect of carbon on the volume fractions and lattice parameters of retained austenite and martensite' *Trans. Am. Inst. Metall. Eng.*, 1953, **197**, 203–204.
15. L. Cheng, A. Böttger, T. H. de Keijser and E. J. Mittemeijer: 'Lattice parameters of iron-carbon and iron-nitrogen martensites and austenites', *Scr. Metall.*, 1990, **24**, 509–514.
16. H. K. D. H. Bhadeshia, S. A. David, J. M. Vitek and R. W. Reed: 'Stress induced transformation to bainite in Fe–Cr–Mo–C pressure vessel steel', *Mater. Sci. Technol.*, 1991, **7**, 686–698.
17. L. Cheng, C. M. Brakman, B. M. Korevaar and E. J. Mittemeijer: 'The tempering of iron-carbon martensite; dilatometric and calorimetric analysis', *Metall. Trans. A*, 1988, **19A**, 2415–2426.